TOXICOLOGICAL SCIENCES **117(1)**, 144–151 (2010)
doi:10.1093/toxsci/kfq189
Advance Access publication July 12, 2010

Primary Endothelial Damage Is the Mechanism of Cardiotoxicity of Tubulin-Binding Drugs

Igor Mikaelian,*[,1] Andreas Buness,† Maria-Cristina de Vera-Mudry,† Charu Kanwal,* Denise Coluccio,* Erik Rasmussen,* Hing W. Char,* Valerie Carvajal,* Holly Hilton,* Juergen Funk,† Jean-Christophe Hoflack,† Mark Fielden,‡ Frank Herting,§ Michael Dunn,* and Laura Suter-Dick†

*Hoffmann-La Roche, Inc., Nutley, New Jersey 07110; †Hoffmann-La Roche, Inc., Basel 4070, Switzerland; ‡Hoffmann-La Roche, Inc., Palo Alto, California 94304; and §Hoffmann-La Roche, Inc., Penzberg D-82377, Germany

[1]To whom correspondence should be addressed. Non-Clinical Safety, Bldg 100/310, Hoffmann-La Roche, Inc., Nutley, NJ 07110. Fax: (973) 235-4710. E-mail: igor.mikaelian@roche.com.

Received March 17, 2010; accepted June 20, 2010

The use of tubulin binders (TBs) in the treatment of cancer often is associated with cardiotoxicity, the mechanism of which has not been elucidated. To test the hypothesis that interstitial cells of the myocardium are the primary target of TBs, we evaluated the acute effects of a single iv administration of three reference TBs: colchicine (0.2 and 2 mg/kg), vinblastine (0.5 and 3 mg/kg), and vincristine (0.1 and 1 mg/kg) 6 and 24 h after dosing. Mitotic arrest was identified at 24 h in all high-dose groups based on an increase in the number of mitotic figures in the interstitium coupled with a decrease in the number of Ki67-positive interstitial cells. Analysis of the myocardial transcriptomic data further supported G2/M cell cycle arrest 6 h after dosing with the high-dose groups of all three compounds. Apoptotic figures and an increase in the number of cleaved caspase 3–positive cells were identified at 6 and 24 h at the highest dose of each compound predominantly in interstitial cells, whereas a few cardiomyocytes were affected as well. Transcriptomic profiling of the myocardium further suggested that some of the affected interstitial cells were endothelial cells based on the upregulation of genes typically associated with vascular damage and downregulation of endothelial cell-specific molecule 1 and apelin. Taken together, these data identify endothelial cells of the myocardium as the primary target of the cardiotoxicity of TBs and identify cell cycle arrest as the mechanism of this toxicity.

Key Words: **heart; cardiotoxicity; cardiac; endothelium; pathogenesis; microtubule.**

Microtubules (MTs) are ubiquitous cytoskeletal fibers that are composed of α,β-tubulin heterodimers bound to MT-associated proteins (Webster, 2002). Chemotherapeutic agents have been used to prevent the incorporation (colchicine, vinblastine, and vincristine) or the release (taxanes [taxol, docetaxel], noscapine) of tubulins from MTs, resulting in G2/M cell cycle arrest and inhibition of cell motility and vesicle trafficking. Indeed, most disruptors of MTs have primarily been used in oncology indications because of their ability to cause a cell cycle arrest. The property of these molecules to also inhibit cell motility and vesicle trafficking has been used for indications where the inhibition of neutrophil function is targeted, including gout, pericarditis, and autoimmune diseases.

The cardiotoxicity in humans induced by agents that inhibit MT assembly has been reported and consists of ischemia, infarction, and ventricular tachycardia in human (Mendis, 1989; Webster, 2002), and impaired intrinsic myocardial contractility in rat (Mery *et al.*, 1994). This cardiotoxicity is not the consequence of a disruption of the contractile function of cardiomyocytes because a functional interaction between MTs and myofibers has not been convincingly demonstrated (Webster, 2002).

We hypothesized that cardiotoxicity induced by tubulin binders (TBs) is the result of a cell cycle arrest that predominantly affects the most labile component of the myocardium, i.e., the endothelial cells of the interstitium. In a first study (Supplementary fig. 1), bromodeoxyuridine immunolabeling showed that mouse and rat hearts contain a population of actively dividing cells, which most likely are endothelial cells, confirming earlier results (Fernandez *et al.*, 2001; Heron and Rakusan, 1995). In a second study, we identified doses of colchicine, vinblastine, and vincristine that cause a histologically detectable increase in mitotic figures in the interstitium of the myocardium (Supplementary table 1). Here, we report gene expression in the myocardium 6 and 24 h after a single dose of colchicine, vinblastine, and vincristine. The transcriptomic data support the hypothesis that inhibitors of tubulin assembly cause endothelial damage. The results of this study may have implications for other oncology drugs that disturb the homeostasis of the highly labile endothelial cells of the myocardium.

MATERIALS AND METHODS

Animals. Male Wistar rats [Crl:Wi(Han)] aged 9 weeks were obtained from Charles River Laboratories (Raleigh, NC) and were acclimated 2 weeks

prior to dosing. Rats were single-housed in polycarbonate solid-bottom cages in a controlled environment (temperature maintained at 22 ± 2°C and humidity at 50 ± 20%) with *ad libitum* access to Purina Certified Rodent Diet 5002-9 (pellets) and reverse osmosis filtered water. All experiments were conducted in accordance to the guidance of the Roche Animal Care and Use Committee.

Treatment and sampling. Vinblastine (0.5 and 3 mg/kg; Sigma-Aldrich, St Louis, MO), vincristine (0.1 and 1 mg/kg; Mayne Pharma, Inc., Lake Forest, IL), and colchicine (0.2 and 2 mg/kg; Sigma-Aldrich) were administered iv in 0.9% saline (six rats per group and time point). These doses were selected based on a previous range-finding study as the highest dose not causing a troponin I (cTnI) increase for the low dose and the lowest dose causing a cTnI increase for the high dose of each compound or the highest dose tested in the preliminary study (Supplementary table 1). Necropsies were performed 6 and 24 h after dosing. At necropsy, the rats were anesthetized with isofluorane/O_2 anesthesia and blood was collected from the retro-orbital sinus for clinical chemistry and hematology. The rats were exsanguinated by catheterization of the abdominal aorta, and a pneumothorax was induced. A sagittal section of the heart running from the base to the apex and across the arch of the aorta was made. The portion of the heart located in the right thorax was fixed in 10% neutral buffered formalin and processed for histology. The other half of the heart ventricular myocardium was stored in RNAlater (Ambion, Austin, TX) at room temperature overnight and then at −70°C until RNA extraction. All the ventricular tissue available was homogenized for RNA extraction.

Histology and clinical pathology. Histology, clinical pathology, and gene expression data were evaluated at all time points for the heart as described previously (Mikaelian *et al*., 2008). Briefly, hematology included erythrocyte count, hemoglobin, hematocrit, red cell distribution, platelets, platelet volume, and total and differential white blood cell count and was performed using the Abbott Cell-Dyn 3500 (Abbott Park, IL). Comprehensive clinical chemistry, including aspartate aminotransferase, creatine kinase, and lactate dehydrogenase, was performed on the Roche/Hitachi Modular Analytics System (Roche Diagnostics, Indianapolis, IN). In addition, cTnI was measured with the Beckman Coulter Access 2 AccuTNI with a lower level of quantification of 0.03 ng/mL (Beckman Coulter, Fullerton, CA). Histopathology was performed on sections stained with hematoxylin-eosin of the organs routinely evaluated in toxicology studies, i.e., the bone (proximal femur and sternum), brain, cecum, colon, duodenum, epididymis, esophagus, ileum, jejunum, kidneys, liver, lung with main-stem bronchi, lymph nodes (mandibular and mesenteric), mammary gland, pancreas, parathyroid glands, pituitary gland, prostate gland, rectum, salivary gland, mandibular, seminal vesicles, skin, spleen, stomach, testes, thymus, thyroid glands, tongue, trachea, and urinary bladder.

Immunohistochemistry. The marker of apoptosis cleaved caspase 3 (rabbit polyclonal Asp175 09661, 1:600; Cell Signaling, Danvers, MA) and the markers of proliferation phospho-histone H3 (mouse monoclonal clone 6G3 9706, 1:2000; Cell Signaling Technology) and Ki67 (rabbit polyclonal Ab-4, 1:2000; Lab Vision, Fremont, CA) were evaluated in the hearts of all rats. The positive events were counted on 10 consecutive ×40 microscopic fields for phospho-histone H3 and Ki67 and 20 consecutive ×40 microscopic fields for the number of mitotic figures, apoptotic figures, and cleaved caspase 3. The effects of the treatments on these parameters were compared using one-way ANOVA.

Gene expression analysis. Hybridization of fragmented *in vitro* transcription product to Rat Genome 230 2.0 Array and washing steps were performed as suggested by the manufacturer (Affymetrix). Each hybridized GeneChip array was scanned with an argon-ion laser scanner at 570 nm (Agilent/Affymetrix). Image analysis was done with the GCOS software (Affymetrix). Quality of the chips was assessed with a variety of analyses. Inspection of the residual images was used to identify potential problems with wet-lab procedures. Signal box plots and glyceraldehyde-3-phosphate dehydrogenase ratios were used to assess RNA quality. In addition, multivariate procedures such as hierarchical clustering and principal components analyses were used to assess the consistency of gene changes for each dose and time condition. All chips passed these quality assessments, and none were dropped from the analysis. Chips were preprocessed using robust multichip analysis (Irizarry et al., 2003) and quantile-quantile normalization. Normalized data were fit to a linear model with dose and time contrasts using the GLM procedure of SAS 9.1 (SAS Institute, Cary, NC). Individual gene mining was performed on the most significantly up- and downregulated genes, as well as for a proposed list of markers for vascular damage. For all transcriptomic data, an absolute value of fold change ≤ 0.67 or ≥ 1.5 and $p \leq 0.05$ identified the level of significance. The data were deposited in the database Gene Expression Omnibus of the National Center for Biotechnology Information under the accession numbers GSE19290 and GSM478817-98. The expression of selected genes was confirmed by qPCR and the data were normalized against Gapdh and Actb (Supplementary data 2 and 3).

RESULTS

Clinical Pathology

Cardiac troponin I concentrations increased significantly after dosing with the high doses of colchicine and vincristine (Table 1). An increase in cTnI was evident after 6 h of dosing with colchicine (five of six rats) and vincristine (two of six rats) and remained elevated after 24 h (six of six rats) for both compounds. Vinblastine caused a significant (> 0.04 ng/ml) increase in cTnI in only one of the six rats at both 6 and 24 h. The increase in cTnI was highest following dosing with colchicine > vincristine > vinblastine.

The other clinical chemistry findings for vinblastine at 3 mg/kg, vincristine at 1 mg/kg, and colchicine at 2 mg/kg consisted of time-dependant increases in alanine aminotransferase, aspartate aminotransferase, alkaline phosphatase, creatine kinase, and/or troponin I and/or decreases in phosphorus, calcium, and potassium. A few of these parameters were occasionally altered in rats at the lower doses. There was also an increase in lactate dehydrogenase for colchicine at 2 mg/kg at 6 h. Treatment-related hematologic findings for vinblastine at 0.5 and 3 mg/kg, vincristine at 1 mg/kg, and colchicine at 2 mg/kg consisted of time- and/or dose-dependent increases in erythrocytes, hemoglobin, hematocrit, platelet volume, and/or neutrophils and/or decreases in platelets, white blood cells, lymphocytes, and eosinophils (Supplementary table 2).

Histology and Immunohistochemistry

There was no evidence of myocardial necrosis on the sections stained with hematoxylin-eosin and phosphotungstic acid hematoxylin-stained sections. There was a time- and dose-dependent increase in the number of mitotic figures, apoptotic figures, and cleaved caspase 3– and phospho-histone H3–positive cells (Table 2; Fig. 1), and these cells almost exclusively were interstitial, with most of them clearly being endothelial cells based on their location lining the vessels. However, a few cardiomyocytes were in mitosis or were positive for phospho-histone H3, especially in the auricles. Standard error for the number of immunopositive cells in each dose group and time point was high, reflecting interindividual variability in the responses among rats. The decrease in the

TABLE 1

Troponin I Concentrations Increased in Male Wistar Rats 6 and 24 h After a Single iv Administration of Colchicine, Vinblastine, and Vincristine. Red-Colored Cells Indicate an Increase in Mean cTnI or in the Number of Rats with cTnI Greater Than or Equal to the Threshold Value 0.04 ng/mL

	Drug		Colchicine		Vinblastine		Vincristine	
Time	Dose (mg/kg)	Vehicle	0.2	2	0.5	3	0.1	1
6 h	Troponin I[a]	BLQ	BLQ	0.86 ± 1.21[b]	BLQ	0.16	BLQ	0.05 ± 0.01
	n^b	0/6	0/6	5/6	0/6	1/6	0/6	2/6
24 h	Troponin I[a]	BLQ	BLQ	0.51 ± 0.64[b]	BLQ	0.06	BLQ	0.13 ± 0.05[b]
	n^b	0/6	0/6	6/6	0/6	1/6	0/6	6/6

Note. BLQ, below quantification.
[a]Mean ± SD.
[b]Number of rats with cTnI $\geq$ 0.04 ng/mL over number of rats tested.

number of Ki67-positive cells that occurred concurrently to the increase of the number of mitotic figures and an increase in phospho-histone H3–positive cells identified a cell cycle arrest.

Histological changes in the other organs occurred for all three drugs and consisted of minimal to marked increased mitotic and apoptotic figures of the proliferating compartments of multiple organs in all animals 6 and 24 h after dosing with vinblastine at 0.5 and 3 mg/kg, vincristine at 1 mg/kg, and colchicine at 2 mg/kg. Similar changes, albeit milder in severity, were present in few rats and few organs for vincristine at 0.1 mg/kg and for colchicine at 0.2 mg/kg. Mitoses were mostly observed at 6 h, whereas apoptotic figures predominated at 24 h. Increased mitotic and/or apoptotic figures were present in epithelial cells of the salivary glands, esophagus, stomach (non-glandular and glandular), small intestine, large intestine, thyroid follicles, pancreatic acini and islets, pituitary gland, seminal vesicles, prostate gland, tongue, interfollicular and follicular keratinocytes, epididymis, liver, and kidney. Increased mitotic and/or apoptotic figures were present in the lymphoid cells of the secondary lymphoid organs, including the lymph nodes (mandibular and mesenteric), spleen, thymus, and gut-associated lymphoid tissues. Increased mitotic and/or apoptotic figures were present in the progenitor compartment of the testis, bone marrow, and subependyma of the brain. Occasionally, mitotic or apoptotic figures were also seen in the lung (bronchiole and alveolar wall) and bone (periosteum and growth plate). A small number of unidentifiable mitotic or apoptotic figures were present in the interstitium of all tissues.

TABLE 2

In the Myocardium, the Administration of Vinblastine, Vincristine, and Colchicine Caused an Increase in Mitotic Figures and Immunolabeling for Phospho-Histone H3 Coupled with a Decrease in Ki67-Positive Cells, Which Indicates a Cell Cycle Arrest. There Was Also an Increase in the Number of Apoptotic Figures and Cleaved Caspase 3–Positive Cells. The Numbers Represent the Mean Values for Each Group, Which Is Followed by SD in Parenthesis. The Cells Were Color Coded to Indicate Increase (red) or a Decrease (blue) in the Parameters Evaluated

	Drug		Saline	Colchicine		Vinblastine		Vincristine	
	Dose (mg/kg)		0	0.2	2	0.5	3	0.1	1
Proliferation	Mitoses (20 HPF[a])	6 h	1 (1)	7 (4)**	2 (3)	10 (5)**	3 (1)*	3 (3)	2 (2)
		24 h	2 (1)	2 (2)	7 (8)	3 (2)	16 (8)***	3 (2)	25 (8)***
	Phospho-histone H3 (10 HPF)	6 h	3 (1)	7 (3)**	3 (2)	15 (9)**	3 (1)	2 (1)	3 (2)
		24 h	3 (2)	3 (1)	8 (5)*	6 (5)	21 (8)***	3 (1)	21 (9)***
	Ki67 (10 HPF)	6 h	228 (68)	161 (64)	156 (49)	197 (54)	191 (36)	135 (29)*	137 (46)*
		24 h	201 (65)	129 (52)	68 (24)***	169 (78)	87 (40) **	162 (31)	81 (27)**
Apoptosis	Apoptotic figures (20 HPF)	6 h	1 (1)	3 (2)	6 (3)**	4 (2)**	6 (3)***	1 (1)	6 (3)***
		24 h	3 (1)	3 (2)	18 (6)***	2 (2)	7 (2)***	2 (2)	13 (4)***
	Cleaved caspase 3 (20 HPF)	6 h	3 (3)	6 (3)	23 (11)**	3 (2)	20 (8)**	2 (2)	20 (22)
		24 h	2 (2)	4 (4)	26 (14)**	2 (1)	7 (5)	8 (4)*	21 (11)**

[a]HPF, high power field (×40).
*$p < 0.05$; **$p < 0.01$; ***$p < 0.001$.

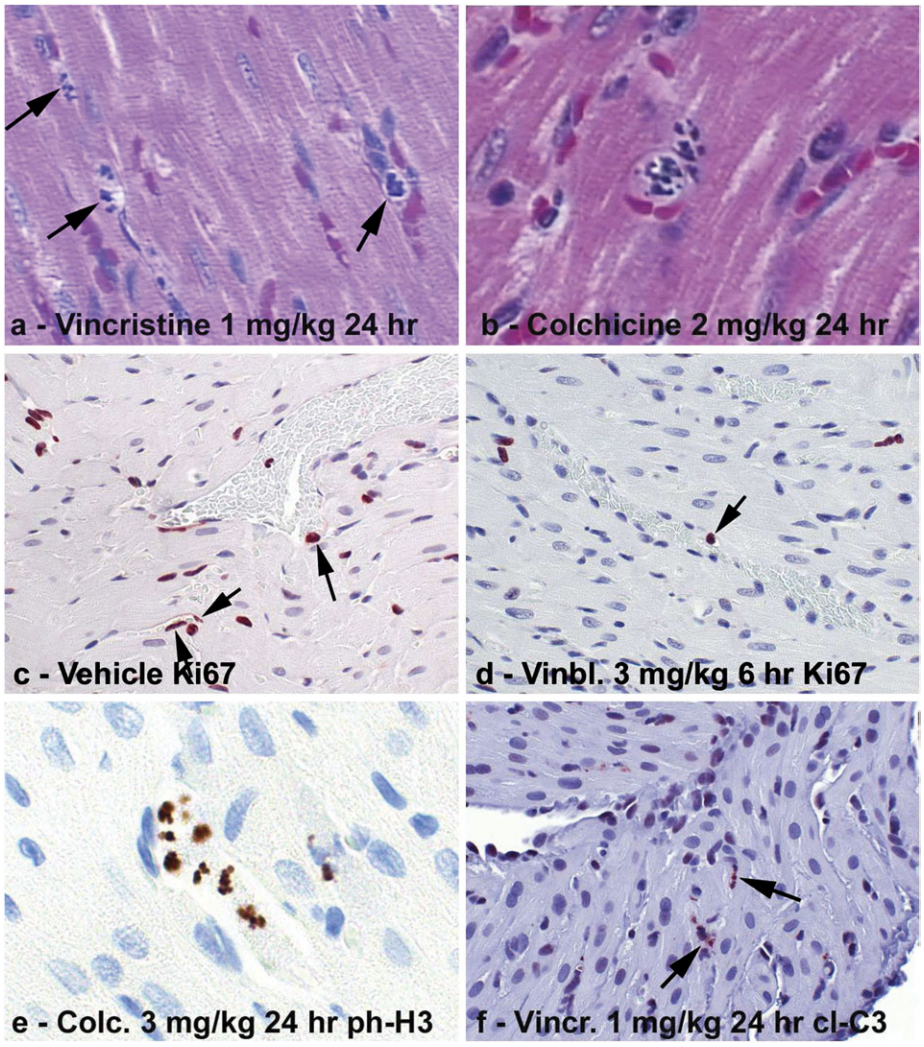

FIG. 1. The administration of the TBs colchicine, vinblastine, and vincristine increased the number of mitotic figures in the interstitium of the myocardium (a). Some mitotic cells clearly were in direct contact with red blood cells (b), a feature consistent with endothelial cells. The increased mitotic rate was associated with a decrease in Ki67 immunolabeling (d) compared with vehicle-treated rats (c), which identified a cell cycle arrest. Some Ki67-positive cells clearly were endothelial cells (c and d, arrows). Although most cells in mitotic arrest were interstitial cells, some were cardiomyocytes, a feature that was best visualized by immunolabeling for phospho-histone H3 (e). Mitotic figures caused by the administration of colchicine, vinblastine, and vincristine often were asymmetrical (a, b, and e) and resulted into apoptosis as identified by immunolabeling for cleaved caspase 3 (f). As for the mitotic figures, many of the apoptotic cells had a linear arrangement (f) and were interpreted as endothelial cells.

Some of these cells may have been endothelial cells, but the number was considerably less than that in the heart.

Transcriptomic Data Overview

Less than 50 probes were significantly changed at the low doses of the three compounds, except for colchicine at 6 h (n = 147 changed probes; Supplementary table 3). This small number of probes is insufficient for transcriptomic analysis. The high doses of the three compounds changed ~350–2700 probes; these numbers were considered appropriate for a transcriptomic analysis. Therefore, the data presented below exclusively describe the high-dose groups. Gene ontology analysis (Table 3 and Supplementary table 4) and Ingenuity Pathway Analysis (IPA) (Supplementary tables 5–7) were dominated by genes associated with tissue damage and inflammation. Also, consistent with myocardial damage, IPA identified a shift from lipid to glucose metabolism (Supplementary table 7), best captured by the identification of a decrease of Fabp3 for all three compounds at 6 h and for vincristine and colchicine at 24 h.

The effects of TBs on the cell cycle were identified by IPA with overrepresentation of the categories "arrest in growth of cells" and "cell cycle progression" at 6 h. Gene ontology analysis supported vascular/endothelial damage, with changes of

TABLE 3

Select Gene Ontology Subcategories Overrepresented in the Transcriptomic Profile of the Heart of Male Wistar Rats 6 and 24 h After a Single iv Administration of a High Dose of Colchicine, Vinblastine, and Vincristine Share Many Commonalities. These Commonalities Indicate Myocardial and Vascular Damage with Inflammation. A Complete List of GO Categories Is Presented in Supplementary table 2

Category	Time	GO subcategories
Biological process	6 h	Angiogenesis, blood vessel morphogenesis, cell proliferation, cytoskeleton, nitric oxide signal transduction, wound healing
	6 and 24 h	Apoptosis, cell death, immune response, inflammatory response, programmed cell death, response to wounding, vasculature development
	24 h	Acute inflammatory response, circulation, muscle development, negative regulation of programmed cell death
Cellular component	6 h	Cytoskeleton
	24 h	Contractile fiber, extracellular matrix, muscle myosin complex, myofibril, sarcomere, structural component of muscle
Molecular function	6 h	Actin binding, cytoskeletal protein binding
	24 h	Actinin binding, structural constituent of muscle

the "angiogenesis", "blood vessel morphogenesis," and "blood vessel development" categories (Supplementary table 4).

Gene Mining

Numerous proposed markers of vascular damage were changed with directionality consistent with vascular/endothelial damage (Table 4). Of importance, the constitutive markers of endothelial cells Esm1 and Apl were downregulated suggesting a decrease in the number of these cells, whereas markers of acute endothelial damage (Woywodt *et al.*, 2008) including Thbs1, Serpine1, Ccl2, S100a8, and S100a9 were upregulated.

The direct pharmacological effect of TBs was identified at the transcriptomic level and consisted of downregulation of numerous probes coding for tubulins (Table 5) and evidence for cell cycle arrest (Table 6). Consistent with cardiomyocyte damage, there was activation of the fetal gene program (Supplementary table 8) and of the p38 mitogen-activated protein kinase (MAPK) pathway and changes of multiple genes involved in fatty acid metabolism (Supplementary table 9).

DISCUSSION

In this study, histology, immunohistochemistry, and transcriptomic data were combined to analyze the cardiotoxic effects of tubulin-binding drugs used in oncology indications. These techniques suggest endothelial cells of the myocardium as an important target of the toxicity of TBs. The same mechanism of endothelial toxicity accounts for part of the efficacy of TBs, which occurs through disruption of the microvasculature in the

TABLE 4

Many Genes Proposed as Markers of Vascular Damage Were Dysregulated in the Myocardium of Rats Dosed with High Doses of Colchicine, Vincristine, and Vinblastine. Values Represent the Fold Change Compared with Controls. Cells Were Color Coded to Identify Upregulated (red: $F \geq 1.5$ and $p \leq 0.05$; pink: $F \geq 1.35$ and $p \leq 0.05$ or $F \geq 2$ and $p \leq 0.10$) and Downregulated (dark blue: $F \leq -1.5$ and $p \leq 0.05$; pale blue: $F \leq -1.35$ and $p \leq 0.05$) Probes. Gene Symbols Are from the Official Nomenclature of the Rat Genome Database

		Colchicine		Vincristine		Vinblastine	
		2 mg/kg		1 mg/kg		3 mg/kg	
Gene symbol	Affy ID	6 h	24 h	6 h	24 h	6 h	24 h
Esm1	1368078_at	−1.8	−1.83	−1.68	−2.67	−1.63	−2.5
Apln	1389651_at		−2.18		−3.10		−2.06
Apln	1368258_at		−1.44		−1.66		−1.46
Vegfa	1370081_a_at				−1.46		−1.42
Ctss	1387005_at						1.42
Cd36	1367689_a_at				1.52		
C3	1373690_at		1.62				
Thbd	1368901_at	1.45				1.35	
Vwf	1389234_at				1.42		1.39
Thbd	1375951_at	1.52				1.37	
Cd44	1387952_a_at		1.83			1.87	
Il6	1369191_at	2.32	1.64				
Cd44	1390659_at		1.82			2.15	
Eprs	1383455_at		1.52		1.49	1.39	
Tfpi2	1377340_at	1.53	2.18			1.8	
Sele	1388018_at	1.43	2.12		1.54	2.03	
Spon1	1373487_at		2.25		2.32	1.61	1.92
F3	1369182_at	2		1.65	1.45	1.42	1.78
Cp	1368420_at	1.29	2.3		2.17	1.55	1.73
Cp	1368418_a_at	1.35	2.34		2.4	1.47	1.78
Il1b	1398256_at	1.43	2.15	1.37	1.82	2.08	1.22
Vcam1	1368474_at	2	1.9	2.05	1.88	2.84	
Ednrb	1387146_a_at		3.64		3.58	1.88	1.89
Fcgr2b	1371079_at		6.11		1.6	3.67	
Plat	1367800_at	2.02	2.7	1.87	2.14	2.34	1.63
Plaur	1387269_s_at	2.41	4.58	1.75	1.73	3.25	
Icam1	1387202_at	2.8	2.99	2.25	1.84	3.25	
Cp	1368419_at	1.47	3.41	1.42	3.56	2.06	2.21
Cd14	1368490_at	2.67	3.44	2.22	4.14	3.26	2.96
Serpine1	1392264_s_at	2.76	5.32	2.78	1.87	5.31	1.51
Spon1	1370312_at	1.52	4.68	1.39	5.84	2.16	4.1
Hmox1	1370080_at	2.49	6.15	1.87	3.12	3.39	2.83
S100a8	1368494_at	5.36	3.31	2.95	2.08	7.94	
Ccl2	1367973_at	4.6	5.56	2.86	3.85	5.67	
Timp1	1367712_at	2.36	8.36	1.85	3.11	5.52	1.51
S100a9	1387125_at	12.24	7.17	6.95	5.9	15.81	2.42
Serpine1	1368519_at	8.56	17.06	7.26	4.58	16.47	2.13
Thbs1	1374529_at	17.03	10.61	13.93	5.54	14.83	1.94
Thbs1	1394109_at	18.09	11.13	14.69	4.93	16.34	

TABLE 5
Treatment with TBs Resulted in Downregulation of Multiple Tubulin Genes. Values Represent the Fold Change Compared with Controls. Cells Were Color Coded to Identify Downregulated (dark blue: $F \leq -1.5$ and $p \leq 0.05$) Probes. Gene Symbols Are from the Official Nomenclature of the Rat Genome Database

		Colchicine		Vinblastine		Vincristine	
		2 mg/kg		3 mg/kg		1 mg/kg	
Gene symbol	Affy ID	6 h	24 h	6 h	24 h	6 h	24 h
Similar to Tuba4	1371542_at	−4.02	−8.52	−8.83	−1.95	−2.82	−5.44
Tubb2	1371390_at	−3.58	−3.01	−6.01		−2.70	−1.72
Tubg1	1370809_at	−2.13	−2.60	−2.63		−1.87	−1.96
Tuba1	1367579_a_at	−2.31	−1.86	−3.82		−2.05	
Tubb5	1387892_at	−1.98	−1.78	−2.81		−1.82	
Tubb5	1370290_at	−1.75	−2.02	−2.63		−1.55	

TABLE 6
Many Genes Involved in Cell Cycle Arrest/Cell Cycle Progression Were Dysregulated in the Myocardium of Rats Dosed with High Doses of Colchicine, Vincristine, and Vinblastine. Values Represent the Fold Change Compared with Controls. Cells Were Color Coded to Identify Upregulated (red: $F \geq 1.5$ and $p \leq 0.05$; pink: $F \geq 1.35$ and $p \leq 0.05$ or $F \geq 2$ and $p \leq 0.10$) and Downregulated (dark blue: $F \leq -1.5$ and $p \leq 0.05$; pale blue: $F \leq -1.35$ and $p \leq 0.05$) Probes. Gene Symbols Are from the Official Nomenclature of the Rat Genome Database

		Colchicine		Vincristine		Vinblastine	
		2 mg/kg		1 mg/kg		3 mg/kg	
Gene symbol	Affy ID	6 h	24 h	6 h	24 h	6 h	24 h
Ak1	1370011_at	−1.36	−2.28		−2.05	−1.41	−1.39
Inha	1387124_at		−2.31		−2.48		−1.42
Aif1	1368558_s_at	−1.49	−1.47			−1.76	
Ak1	1389185_at		−2.60		−1.97		
Gas7	1370963_at	−1.54		−1.46		−1.48	
Cdkn3	1372685_at		−1.54				−1.44
Cdkn1a	1387391_at				1.61		
Plagl1	1387122_at	1.52				1.41	
Sesn1	1372248_at	1.96		1.50			
Sesn1	1395809_at	2.13		1.72			
Nbn	1387977_at		1.75		1.76	1.57	1.44
Cdkn1a	1388674_at	1.62	1.85		1.54		1.63
Tpd52l1	1372626_at		2.43		2.83		1.70
Rassf1	1373989_at	1.81	1.72	1.42	1.36	1.68	
Myd116	1370174_at	2.45	2.37	1.77	1.55	2.36	
Gadd45a	1368947_at	2.25	2.69	1.67	1.76	2.42	
Gadd45b	1372016_at	3.06	1.81	1.97	1.47	2.54	
Gadd45g	1388792_at	2.11	4.10		2.40	2.37	1.56
Myc	1368308_at	2.65	9.20	2.23	3.03	4.01	

tumors (Kanthou *et al.*, 2004). Importantly, in organs other than the heart, endothelial cells were not affected by cell cycle arrest. This difference in sensitivity to TBs of endothelial cells of the heart and of the other tissues likely is the result of a difference in the proliferation rate of these different populations of endothelial cells because endothelial cells of the heart have a high proliferation rate (Fernandez *et al.*, 2001; Heron and Rakusan, 1995).

These observations are important because they indicate a liability for the endothelium of the heart and subsequently of the myocardium as a whole for drugs targeting the cell cycle or actively proliferating endothelial cells. Cell cycle arrest and apoptosis were present in organs other than the heart with a distribution consistent with the literature: These changes were prominent in the parenchymal cells in organs, such as the liver and kidney, the epithelial cells in all tissues, the proliferating compartment of the bone marrow and lymphoid organs, and the testis. However, endothelial changes were not prominent in these tissues.

The identification of the mechanism of cardiotoxicity of TBs through a primary effect on the endothelial cells of the heart has implications for antiangiogenic compounds, especially because cardiotoxicity has been identified in the clinic with some of these compounds (Schmidinger *et al.*, 2008). Thorough histomorphological and transcriptomic evaluation of the early time points following the administration of antiangiogenic compounds is warranted to determine whether their cardiotoxicity is the result of a primary endothelial effect or a separate mechanism of cardiotoxicity.

There was no microscopic evidence of cardiomyocyte damage in spite of alterations in cTnI and transcriptomic markers consistent myocardial damage. These markers included increases of cTnI concentrations and activation/upregulation of the fetal gene program (Hwang *et al.*, 2002; Izumo *et al.*, 1988); the p38 MAPK pathway (Wold *et al.*, 2005; Zhu *et al.*, 1999); a shift from fatty acid to glucose metabolism (Aasum *et al.*, 2003; Barger and Kelly, 1999; Strøm *et al.*, 2005); and of multiple gene categories associated with inflammation and cell death identified by gene set analysis using IPA, gene ontology, and in-house lists of markers (Mikaelian *et al.*, 2008). The absence of myocardial necrosis or of prominent changes in cardiomyocytes highlights the limitation of histopathology to identify cardiomyocyte damage after a single administration of a mild cardiotoxicant such as the three compounds tested in this study. This observation also supports the use of transcriptomics to more reliably predict cardiotoxicity in man than histopathology. Also, discrepancies between the microscopic evaluation and increases of cTnI concentrations may be because of the use of ultrasensitive analytical methods for cTnI.

Transcriptomic analysis identified the mechanism of cardiotoxicity of TBs, i.e., primary endothelial damage, because early time points were evaluated. As exemplified in this study, it is important that the time points for transcriptomics studies capture the very early stages of cardiotoxicity because the

repertoire of responses of the heart to injury is limited to hypertrophy and fibrosis as the end points of many insults, regardless of the initial pathophysiology.

Cell cycle arrest was among the gene categories identified by GO and IPA analyses and was confirmed histologically and immunohistochemically. The identification of alterations of the cell cycle and of tubulin homeostasis at the transcriptomic level required gene set analysis mining, which is inherently subjective. The evaluation of the transcriptomic profile of other compounds causing cell cycle arrest, e.g., other taxanes, cyclin, or aurora kinase inhibitors, is needed to establish a more comprehensive signature for endothelial cell cycle arrest in the heart.

There is a need to identify blood markers of endothelial damage in the peripheral blood. We evaluated the transcriptomic profile of the peripheral blood of the rats from this study and found that endothelial cell–specific genes, in particular Esm1, Apln, and Plau, were not enriched at any of the time points evaluated (unpublished data). Possible causes for this negative observation include dilution of the endothelial cell–specific transcripts in the blood, decreased expression of endothelial cell–specific transcripts in these damaged cells, and the rapid clearance from the blood of damaged endothelial cells. Indeed, the prevailing hypothesis regarding apoptotic endothelial cells is that very few of them reach the circulation because they are rapidly cleared from the blood (Woywodt *et al.*, 2008). In the peripheral blood, protein-based assays may more reliably identify an endothelial damage than transcriptomics. However, blood collection techniques may also interfere with the assay because endothelial cells from the venipuncture site may contaminate the sample and thereby compromise the identification of any treatment-related increase in the number of circulating endothelial cells and their fragments.

Similarly, enrichment of the transcripts of circulating endothelial progenitor cells (CEPCs) may provide an indication of endothelial damage. Except for Ccr1, the other markers of CEPCs were not overexpressed in the peripheral blood at any time point (unpublished data), including the recently identified markers Anxa5, Mcam, Pecam, Edn1, Ifi30, Vwf, Itgad, Kdr, and Mmp2 (Thomas *et al.*, 2009). The increase in Ccr1 in the absence of any increase in other markers of CEPCs in this study was interpreted as the result of neutrophilia and not as the result of an increase in the number of CEPCs because Ccr1 is also expressed by neutrophils. The absence of an enrichment of the transcripts of CEPCs may be related to their low numbers in the circulating blood.

It is generally accepted that mitotic arrest caused by TBs causally results in apoptosis (Jordan *et al.*, 1996; Woods *et al.*, 1995; Ye *et al.*, 2001). In this study, there was no clear temporal relationship between the mitotic arrest and apoptosis as assessed by microscopic and immunohistochemical evaluation. Possible explanations for this absence of temporal relationship includes the variability of response between individual rats as indicated by a broad SD for all microscopic parameters evaluated, the inability to follow temporally these parameters in an individual rat, and the dose and time selections for this study. Also, the increase in mitoses and/or phospho-histone H3–positive cells occurred at 6 h with the low doses of colchicine and vinblastine but at 24 h with the high doses of these compounds. The cause for this observation is not known.

In conclusion, our work established that TBs exert a specific toxicity toward endothelial cells of the heart, presumably because these cells have a high turnover. These findings have important implications for other oncology drugs targeting angiogenesis and cell cycling.

SUPPLEMENTARY DATA

Supplementary data are available online at http://toxsci.oxfordjournals.org/.

FUNDING

Hoffmann-La Roche, Inc.

ACKNOWLEDGMENTS

Dr Isabelle Wells developed the Hoffmann-La Roche, Inc., proprietary software "GoSubTree." Dr Kyle Kolaja provided constructive criticism in the review of the manuscript. Conflict of Interest: All authors are current or past employees of Hoffmann-La Roche, Inc.

REFERENCES

Aasum, E., Hafstad, A. D., and Larsen, T. S. (2003). Changes in substrate metabolism in isolated mouse hearts following ischemia-reperfusion. *Mol. Cell Biochem.* **249,** 97–103.

Barger, P. M., and Kelly, D. P. (1999). Fatty acid utilization in the hypertrophied and failing heart: molecular regulatory mechanisms. *Am. J. Med. Sci.* **318,** 36–42.

Fernandez, E., Siddiquee, Z., and Shohet, R. V. (2001). Apoptosis and proliferation in the neonatal murine heart. *Dev. Dyn.* **221,** 302–310.

Heron, M. I., and Rakusan, K. (1995). Proliferating cell nuclear antigen (PCNA) detection of cellular proliferation in hypothyroid and hyperthyroid rat hearts. *J. Mol. Cell Cardiol.* **27,** 1393–1403.

Hwang, J. J., Allen, P. D., Tseng, G. C., Lam, C. W., Fananapazir, L., Dzau, V. J., and Liew, C. C. (2002). Microarray gene expression profiles in dilated and hypertrophic cardiomyopathic end-stage heart failure. *Physiol. Genomics* **10,** 31–44.

Irizarry, R. A., Hobbs, B., Collink, F., Beazer-Barclay, Y. D., Antonellis, K. J., Scherf, U., and Speed, T. P. (2003). Exploration, normalization, and summaries of high density oligonucleotide array probe level data. *Biostatistics* **4,** 249–264.

Izumo, S., Nadal-Ginard, B., and Mahdavi, V. (1988). Protooncogene induction and reprogramming of cardiac gene expression produced by pressure overload. *Proc. Natl. Acad. Sci. U.S.A.* **85,** 339–343.

Jordan, M. A., Wendell, K., Gardiner, S., Derry, W. B., Copp, H., and Wilson, L. (1996). Mitotic block induced in HeLa cells by low concentrations of paclitaxel (Taxol) results in abnormal mitotic exit and apoptotic cell death. *Cancer Res.* **56,** 816–825.

Kanthou, C., Greco, O., Stratford, A., Cook, I., Knight, R., Benzakour, O., and Tozer, G. (2004). The tubulin-binding agent combretastatin A-4-phosphate arrests endothelial cells in mitosis and induces mitotic cell death. *Am. J. Pathol.* **165,** 1401–1411.

Mendis, S. (1989). Colchicine cardiotoxicity following ingestion of Gloriosa superba tubers. *Postgrad. Med. J.* **65,** 752–755.

Mery, P., Riou, B., Chemla, D., and Lecarpentier, Y. (1994). Cardiotoxicity of colchicine in the rat. *Intensive Care Med.* **20,** 119–123.

Mikaelian, I., Coluccio, D., Morgan, K. T., Johnson, T., Ryan, A. L., Rasmussen, E., Nicklaus, R., Kanwal, C., Hilton, H., Frank, K., *et al.* (2008). Temporal gene expression profiling indicates early up-regulation of interleukin-6 in isoproterenol-induced myocardial necrosis in rat. *Toxicol. Pathol.* **36,** 256–264.

Schmidinger, M., Zielinski, C. C., Vogl, U. M., Bojic, A., Bojic, M., Schukro, C., Ruhsam, M., Hejna, M., and Schmidinger, H. (2008). Cardiac toxicity of sunitinib and sorafenib in patients with metastatic renal cell carcinoma. *J. Clin. Oncol.* **26,** 5204–5212.

Strøm, C. C., Aplin, M., Ploug, T., Christoffersen, T. E., Langfort, J., Viese, M., Galbo, H., Haunso, S., and Sheikh, S. P. (2005). Expression profiling reveals differences in metabolic gene expression between exercise-induced cardiac effects and maladaptive cardiac hypertrophy. *FEBS J.* **272,** 2684–2695.

Thomas, R. A., Pietrzak, D. C., Scicchitano, M. S., Thomas, H. C., McFarland, D. C., and Frazier, K. S. (2009). Detection and characterization of circulating endothelial progenitor cells in normal rat blood. *J. Pharmacol. Toxicol. Methods* **60,** 263–274.

Webster, D. R. (2002). Microtubules in cardiac toxicity and disease. *Cardiovasc. Toxicol.* **2,** 75–89.

Wold, L. E., Aberle, N. S., II., and Ren, J. (2005). Doxorubicin induces cardiomyocyte dysfunction via a p38 MAP kinase-dependent oxidative stress mechanism. *Cancer Detect. Prev.* **29,** 294–299.

Woods, C. M., Zhu, J., McQueney, P. A., Bollag, D., and Lazarides, E. (1995). Taxol-induced mitotic block triggers rapid onset of a p53-independent apoptotic pathway. *Mol. Med.* **1,** 506–526.

Woywodt, A., Kirsch, T., and Haubitz, M. (2008). Circulating endothelial cells in renal disease: markers and mediators of vascular damage. *Nephrol. Dial. Transplant.* **23,** 7–10.

Ye, K., Zhou, J., Landen, J. W., Bradbury, E. M., and Joshi, H. C. (2001). Sustained activation of p34(cdc2) is required for noscapine-induced apoptosis. *J. Biol. Chem.* **276,** 46697–46700.

Zhu, W., Zou, Y., Aikawa, R., Harada, K., Kudoh, S., Uozumi, H., Hayashi, D., Gu, Y., Yamazaki, T., Nagai, R., *et al.* (1999). MAPK superfamily plays an important role in daunomycin-induced apoptosis of cardiac myocytes. *Circulation* **100,** 2100–2107.